Received: 18 March 2020 | Revised: 13 August 2020 | Accepted: 31 August 2020

DOI: 10.1002/jimd.12312

ORIGINAL ARTICLE

JIMD SSIEM WILEY

The phenotype associated with variants in *TANGO2* may be explained by a dual role of the protein in ER-to-Golgi transport and at the mitochondria

Miroslav P. Milev[1] | **Djenann Saint-Dic**[1] | **Khashayar Zardoui**[1] | **Thomas Klopstock**[2,3,4] | **Christopher Law**[5] | **Felix Distelmaier**[6] | **Michael Sacher**[1,7]

[1]Department of Biology, Concordia University, Montreal Quebec, Canada

[2]Department of Neurology, Friedrich-Baur-Institute, Ludwig-Maximilians-University, Munich, Germany

[3]German Center for Neurodegenerative Diseases (DZNE), Munich, Germany

[4]Munich Cluster for Systems Neurology (SyNergy), Munich, Germany

[5]Centre for Microscopy and Cellular Imaging, Concordia University, Quebec, Canada

[6]Department of General Pediatrics, Neonatology and Pediatric Cardiology, University Children's Hospital Düsseldorf, Medical faculty, Heinrich Heine University, Düsseldorf, Germany

[7]Department of Anatomy and Cell Biology, McGill University, Quebec, Canada

Correspondence
Felix Distelmaier, Department of General Pediatrics, Neonatology and Pediatric Cardiology, University Children's Hospital Duesseldorf, Heinrich Heine University, Moorenstr. 5, D-40225 Duesseldorf, Germany.
Email: felix.distelmaier@med.uni-duesseldorf.de

Michael Sacher, Concordia University, Department of Biology, 7141 Sherbrooke Street West SP-457.01, Montreal, QC H4B1R6, Canada.
Email: michael.sacher@concordia.ca

Funding information
Bundesministerium für bildung und forschung (BMBF); Canadian Institutes of Health Research; Deutsche Forschungsgemeinschaft; Natural Sciences and Engineering Research Council of Canada

Communicating Editor: Manuel Schiff

Abstract

TANGO2 variants result in a complex disease phenotype consisting of recurrent crisis-induced rhabdomyolysis, encephalopathy, seizures, lactic acidosis, hypoglycemia, and cardiac arrhythmias. Although first described in a fruit fly model as a protein necessary for some aspect of Golgi function and organization, its role in the cell at a fundamental level has not been addressed. Such studies are necessary to better counsel families regarding treatment options and nutrition management to mitigate the metabolic aspects of the disease. The few studies performed to address the pathway(s) in which TANGO2 functions have led to enigmatic results, with some suggesting defects in membrane traffic while others suggest unknown mitochondrial defects. Here, we have performed a robust membrane trafficking assay on fibroblasts derived from three different individuals harboring TANGO2 variants and show that there is a significant delay in the movement of cargo between the endoplasmic reticulum and the Golgi. Importantly, this delay was attributed to a defect in TANGO2 function. We further show that a portion of TANGO2 protein localizes to the mitochondria through a necessary but not sufficient stretch of amino acids at the amino terminus of the protein. Fibroblasts from affected individuals also displayed changes in mitochondrial morphology. We conclude that TANGO2 functions in both membrane trafficking and in some as yet

Felix Distelmaier and Michael Sacher contributed equally to this study.

undetermined role in mitochondria physiology. The phenotype of affected individuals can be partially explained by this dual involvement of the protein.

KEYWORDS

cardiac arrhythmia, Golgi, membrane traffic, mitochondria, rhabdomyolysis, TANGO2

1 | INTRODUCTION

Mutations in *TANGO2* (transport and Golgi organization 2 homolog) were recently described as a cause of a childhood-onset neurometabolic disease (OMIM # 616878).[1,2] The clinical course is characterized by recurrent metabolic crises with severe rhabdomyolysis, encephalopathy, seizures, lactic acidosis, hypoglycemia, and cardiac arrhythmias. Episodes are typically triggered by febrile infections, leading to irreversible brain damage and neurological deterioration. Prognosis is unfavorable with significant disability and early death in many of the affected individuals. So far, no therapeutic options are available.

Very little is known about TANGO2 from a fundamental standpoint. The gene name refers to a genetic screen that was conducted in *Drosophila* and reported nearly 15 years ago.[3] The hits in this screen were given the name TANGO for transport and Golgi organization. The screen identified 20 genes whose depletion by RNA interference resulted in a defect in secretion of a marker protein that utilizes the endomembrane system. The hits in this screen were then assigned to four different groups depending on whether they had an effect (classes A-C) or not (class D) on Golgi membranes. The relevance of the screen to protein sorting was solidified by the identification of a SNARE protein (Use1) and by a subsequent study demonstrating that TANGO1 functions in collagen secretion at the level of the endoplasmic reticulum (ER).[4] TANGO2 was placed into the class A grouping of genes whose products affect the localization of Golgi enzymes, resulting in their redistribution to the ER. It is noteworthy that this study examined only a single Golgi enzyme (mannosidase II), so the overall morphology of the Golgi following depletion of this protein is not known. Interestingly, knockdown of genes involved in fatty acid and cholesterol metabolism also resulted in a class A phenotype suggesting that these pathways may influence membrane traffic.

The little that is known about mammalian TANGO2 comes from reports of individuals with TANGO2 deficiency and from a single study of several mouse proteins including the TANGO2 homolog called T10. The mouse study used crude membrane fractionation to demonstrate that T10 was a mitochondrial protein that was readily released from this organelle upon sonication, suggesting that it is not a membrane protein.[5] Studies on humans harboring variants in TANGO2 have revealed subtle or no effects on Golgi morphology or membrane trafficking.[1,2,6,7] One study addressed localization of the protein but concluded that it does not localize to either the Golgi or the mitochondria.[6] Interestingly, some of these reports suggest the protein plays a role in mitochondrial physiology but it is unclear how the protein is affecting this organelle.

The controversy regarding TANGO2 localization and function is also reflected by the clinical picture, which combines features of a fatty acid metabolism disorder and a mitochondrial disease. The combination of metabolic crises with severe rhabdomyolysis, hypoglycemia and cardiac arrhythmia seen in individuals with TANGO2 variants is reminiscent of carnitine palmitoyltransferase 2 deficiency.[8]Neurological deterioration with regression and seizures as well as episodes with lactic acidosis are suggestive of a respiratory chain disorder. As a consequence, counseling of affected families regarding treatment options and nutrition management is extremely difficult.

Based on these discrepancies, we aimed to gain further insights into the cellular localization of human TANGO2 and to determine which cellular processes are affected by the loss of the protein. Our data revealed that, while the majority of TANGO2 is found within the cytoplasm, a portion is found to associate with mitochondria. The mitochondrial localization is dependent upon an amino-terminal sequence on the protein, and loss of TANGO2 affects overall mitochondrial morphology. In addition, our data demonstrate that a defect in ER-to-Golgi traffic in cells that are devoid of TANGO2 can be rescued by the wild type protein. Collectively, our data suggest that TANGO2 affects two cellular processes and we discuss how each may explain the complex clinical phenotype.

2 | METHODS

2.1 | Fibroblasts used in this study

The fibroblasts used in this study were derived from individuals harboring variants in TANGO2 that were previously described.[1] In the present study, subjects 1-3 (S1-S3) have the following variants, respectively: homozygous c.418C>T (resulting in a premature stop codon);

homozygous c.(56+1_57-1)_(*1_?)del; exon 3-9 del and exon 6 del.

2.2 | Immunoblotting

Cells were lysed using CelLytic M reagent with protease inhibitors (Sigma-Aldrich, St. Louis, MO) for the gels in Figures 1 and S1, or with a lysis buffer containing 50 mM Tris, pH 7.2, 150 mM NaCl, 0.5 mM EDTA, 1 mM DTT, 0.5% Triton X-100 [vol/vol], protease inhibitor cocktail (Roche) and PhosStop (Roche) for the gel in Figure 2. A total of 30-40 μg of whole cell lysate was loaded and separated in either a 12% Bis/Tris polyacrylamide gel using MES running buffer or a 12% Tris/glycine gel. After electrophoresis, the gels were transferred to nitrocellulose membranes. Membranes were blocked with 3% skim milk powder in TBS with 0.1% Tween 20 for 1 hour and incubated with primary antibodies that recognized: TANGO2 (rabbit; Proteintech, Rosemont, IL); GAPDH (mouse; ThermoFisher, Waltham, MA); p115 (mouse; kind gift from Dr. Martin Lowe, University of Manchester); TOM20 (mouse; Santa Cruz Biotechnologies); tubulin (mouse; Sigma, St. Louis, MO); TRAP-α (rabbit; kind gift from Manu Hegde, MRC Laboratory). Incubations were performed overnight at 4°C. After washing, membranes were incubated with horseradish peroxidase-conjugated anti-rabbit IgG or anti-mouse IgG (Amersham, Little Chalfont, UK) as secondary antibodies for 1 hour at room temperature and then treated with either BM Chemiluminescence blotting substrate (Roche, Basel, Switzerland), Evolution Borealis plus Western Blot Detection System (Montreal Biotech Inc., Canada) or MilliporeSigma Immobilon Western Chemiluminescent HRP Substrate (ThermoFisher Scientific, USA).

2.3 | Small interfering RNA (siRNA)

For siRNA depletion of TANGO2, cells were transfected using 22 nM SilencerSelect siRNA (Tango2 ID s43376, Tango2 ID s43378; Ambion) or a negative control siRNA (siRNA #2 [negative control]; Ambion) and Lipofectamine RNAiMAX (Invitrogen) according to the manufacturer's protocol on 6-well plates (100 000 cells/well). siRNA was added on days 1, 4, and 7 of cell culturing. On day 9, cells were lysed. Western blotting was performed as described above.

2.4 | Stable cell line generation

Stable TANGO2-RFP neomycin-resistant and Mito-YFP hygromycin-resistant cell lines were generated in HeLa cells. Briefly, HeLa cells were plated in 10 cm dishes at 60% confluency. The following day the cells were transfected with 2 μg of plasmid DNA using JetPRIME transfection reagent (Polyplus Transfection, New York, NY). Twenty-four hours post-transfection, 500 μg/mL G418 (Invitrogen, Carlsbad, CA) or 200 μg/mL Hygromycin was added to the medium for selection. Two days later the cell cultures were sub-cultured at lower densities. Resistant monoclonal cell lines were isolated 10 days following selection.

2.5 | Retention using selective hooks assay

The retention using selective hooks (RUSH) assay was performed as previously described.[9] Briefly, cells were transfected by electroporation with a plasmid expressing one of the Golgi-localized enzymes (sialyl transferase-GFP fused to streptavidin binding protein or mannosidase II-RFP fused to streptavidin binding protein). In both cases, the plasmid also expressed KDEL-tagged streptavidin for ER retention, thus retaining the reporter proteins in the ER. Release of the reporter from the ER was accomplished by addition of 40 μM biotin and live cells were monitored by fluorescence microscopy. Quantification was performed as described in Milev et al.[10] Images were obtained on a Nikon Livescan sweptfield confocal microscope with a ×40 objective lens (NA 0.95).

2.6 | Immunofluorescence microscopy

Cells were grown in DMEM medium supplemented with 10% fetal bovine serum. Fixation and staining of the cells were performed as previously described[11] Cells were imaged on a Nikon C2 laser scanning confocal microscope with a ×60 objective lens (NA 1.49). Secondary antibodies were goat anti-mouse AlexaFluor488 and goat anti-rabbit AlexaFluor647 (Life Technologies, Carlsbad, CA).

2.7 | Mitochondrial morphology measurements

Cells were fixed and stained with mouse anti-TOM20 IgG (Santa Cruz Biotechnologies) and imaged as above. A custom macro script for Image J patterned after that of Valente et al[12] was used to measure the parameters shown in Figure 3. Values are displayed with the *SE* of the mean. Briefly, the investigator delineates the boundaries of cells based on the TOM20 signal, then

thresholding is performed and the resulting thresholded objects were analyzed on a per-cell basis.

2.8 | Molecular biological techniques and antibodies

Standard techniques for DNA amplification and cloning were employed. The canonical TANGO2 isoform (Uniprot ID Q6ICL3-1) was cloned into the plasmids pmRFP1-N1 and pmRFP1-C1 (Addgene, Watertown, MA) using HindIII and BamHI restriction endonuclease sites. The DNA sequence encoding the amino-terminal 40 residues of TANGO2 was synthesized by Integrated DNA Technologies (Coralville, IA).

2.9 | Subcellular fractionation

Fractionation of fibroblasts into mitochondrial and cytosolic fractions was performed as described.[13]The final mitochondrial pellet was resuspended in the same volume as the cytosol and equal volumes were loaded onto an SDS-polyacrylamide gel for western analysis.

2.10 | Assessing mitochondrial and cytosolic TANGO2 levels

Quantitative analysis of the ratio of mitochondrial compared to non-mitochondrial fluorescence intensity was performed for RFP-fused TANGO2 constructs transfected into HeLa cells stably expressing Mito-YFP. Fluorescence intensities for mitochondrial and cytoplasmic areas were measured using an ImageJ macro and the ratio of mitochondrial compared to non-mitochondrial intensity was plotted. Briefly, an observer outlined individual cells and their nuclei on a summed Z-projection, a mask of mitochondria was made by selecting a single cell and performing Otsu's threshold detection method upon it. The cytosol was then defined as the user-outlined cell minus the nucleus and the mitochondria. The mean intensity and area of each of these regions was then measured in the summed Z-projection.

3 | RESULTS

3.1 | The absence of TANGO2 affects membrane traffic without affecting Golgi morphology

Given that TANGO2 was reported to function in membrane trafficking yet variants in the gene lead to clinical features that are reminiscent of a mitochondrial defect, we sought to clarify where the protein functions in a cell. For these studies we used fibroblasts derived from three different individuals harboring TANGO2 variants[1] (also see Section 2.1).

The cells used do not express detectable amounts of TANGO2 (Figures 1A and S1). We first examined the morphology of the Golgi by staining the cells for several Golgi makers including p115 and mannosidase II. We included the latter Golgi enzyme since it was reported that in *Drosophila*, mannosidase II redistributes to the ER upon deletion of TANGO2.[3] We did not detect any difference in localization of the two Golgi marker proteins in any of the fibroblasts from the affected individuals compared to control (Figure 1B). A closer assessment using three-dimensional reconstruction of the Golgi from Z-stacks did not reveal any obvious morphological differences in the Golgi between control and affected individuals (Figure S2).

We next examined the transport of protein from the ER to the Golgi using the RUSH assay.[9] In this assay, a fluorescently labeled cargo protein (two different Golgi enzymes were used) is retained in the ER and released upon addition of biotin. The accumulation of the cargo in the Golgi is then followed over time and quantified. While control showed a steady increase in Golgi fluorescence over the time course of the assay, fibroblasts from all three affected individuals showed a striking delay in transport of both cargo proteins to the Golgi (Figures 1C-F and S3). Importantly, expression of wild type canonical TANGO2 (Uniprot ID Q6ICL3-1) was able to rescue the membrane trafficking defect of the ST-GFP cargo, indicating that it is due to the absence of the TANGO2 protein. Collectively, our data suggest that while the absence of TANGO2 does not affect Golgi morphology, it does result in a significant delay in ER-to-Golgi transport.

3.2 | A portion of TANGO2 localizes to mitochondria

Given that TANGO2 was affecting ER-to-Golgi transport yet did not affect Golgi morphology, we sought to determine the localization of the protein. The commercially available antibody that we used was not sufficient to give a reproducible result by immunofluorescence staining, consistent with what was stated by others.[6] Therefore, we tagged the protein with monomeric red fluorescent protein (mRFP1) at both the carboxy- (TANGO2-RFP) and amino-terminus (RFP-TANGO2). We first fractionated the cells into mitochondrial-enriched and cytosolic fractions. It should be noted that each fraction also contained other cellular compartments such as the ER (marked by

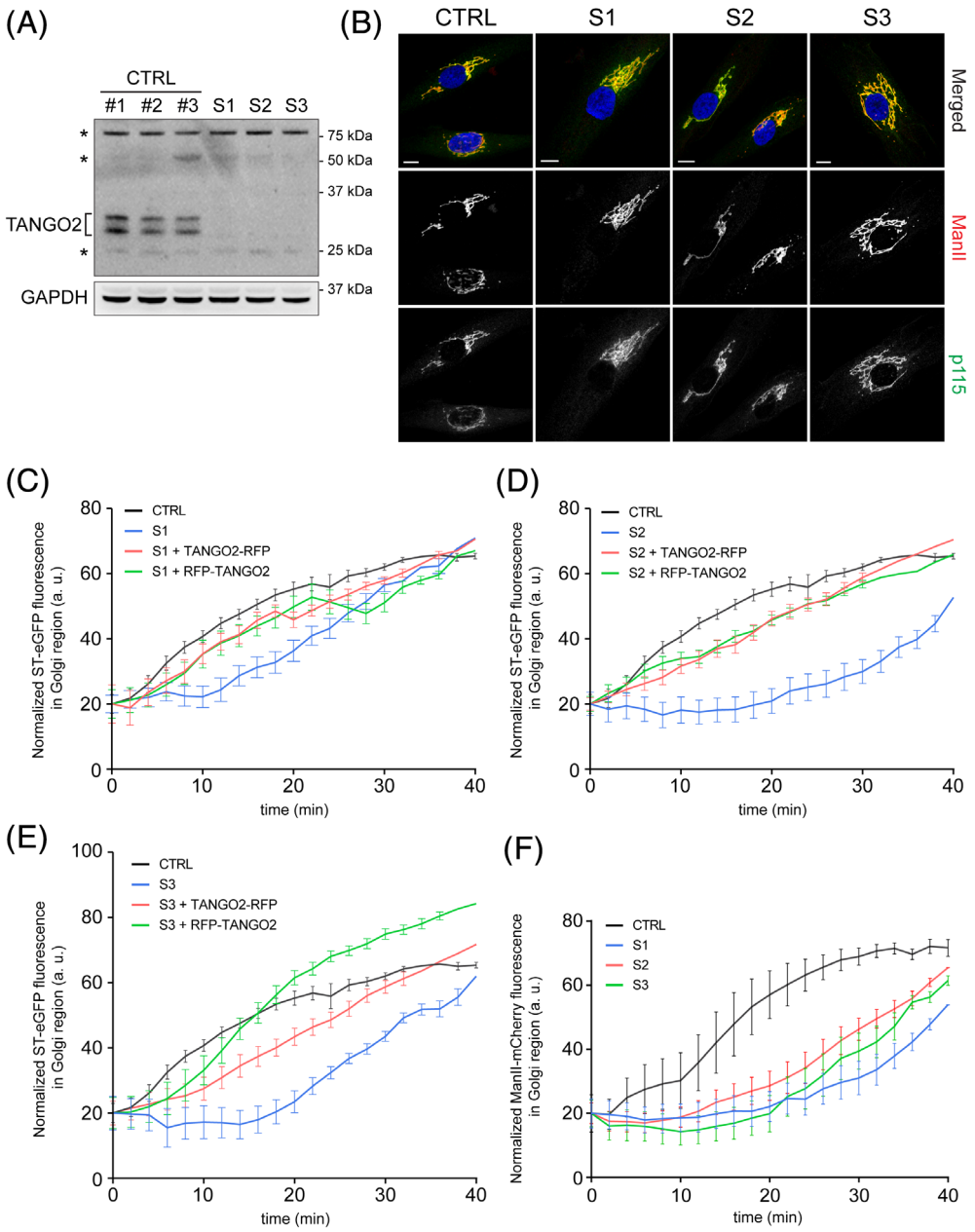

FIGURE 1 Fibroblasts from subjects with TANGO2 variants show a TANGO2-dependent defect in ER-to-Golgi traffic. A, Lysates of fibroblasts derived from subjects 1-3 as well as three different controls were prepared and probed for TANGO2 and GAPDH (as a loading control) by western analysis. TANGO2 bands are indicated to the left of the panel. Bands with an asterisk (*) are cross-reactive polypeptides since they do not disappear upon RNA interference. B, Fibroblasts from subjects 1-3 as well as control were fixed and stained with anti-mannosidase II (red channel) or anti-p115 (green channel), as indicated. Hoechst (blue channel) was included to reveal the nucleus. The scale bars represent 10 μm. C-F, The RUSH assay was performed with ST-GFP on control fibroblasts (black curves) and fibroblasts from subjects 1, C; 2, D; 3, E, or with mannosidase II-mCherry on all three subjects, F. In panels C-E, the blue curves represent the untransfected fibroblasts while the red and green curves represent fibroblasts that were transfected with either TANGO2-RFP or RFP-TANGO2, respectively. Representative images from the movies are shown in Figure S3

TRAP-α) and the Golgi (marked by p115). We probed the fractions for the presence of TANGO2 (endogenous) and transfected TANGO2-RFP or RFP-TANGO2, along with markers for each fraction (tubulin for the cytosol, and TOM20 for the mitochondria). As shown in Figure 2A, although the vast majority of endogenous TANGO2 was found in the cytosol, a small but reproducible amount was found in the mitochondrial-enriched fraction. The results were similar for the TANGO2-RFP and RFP-TANGO2, though more of the fusion protein was found

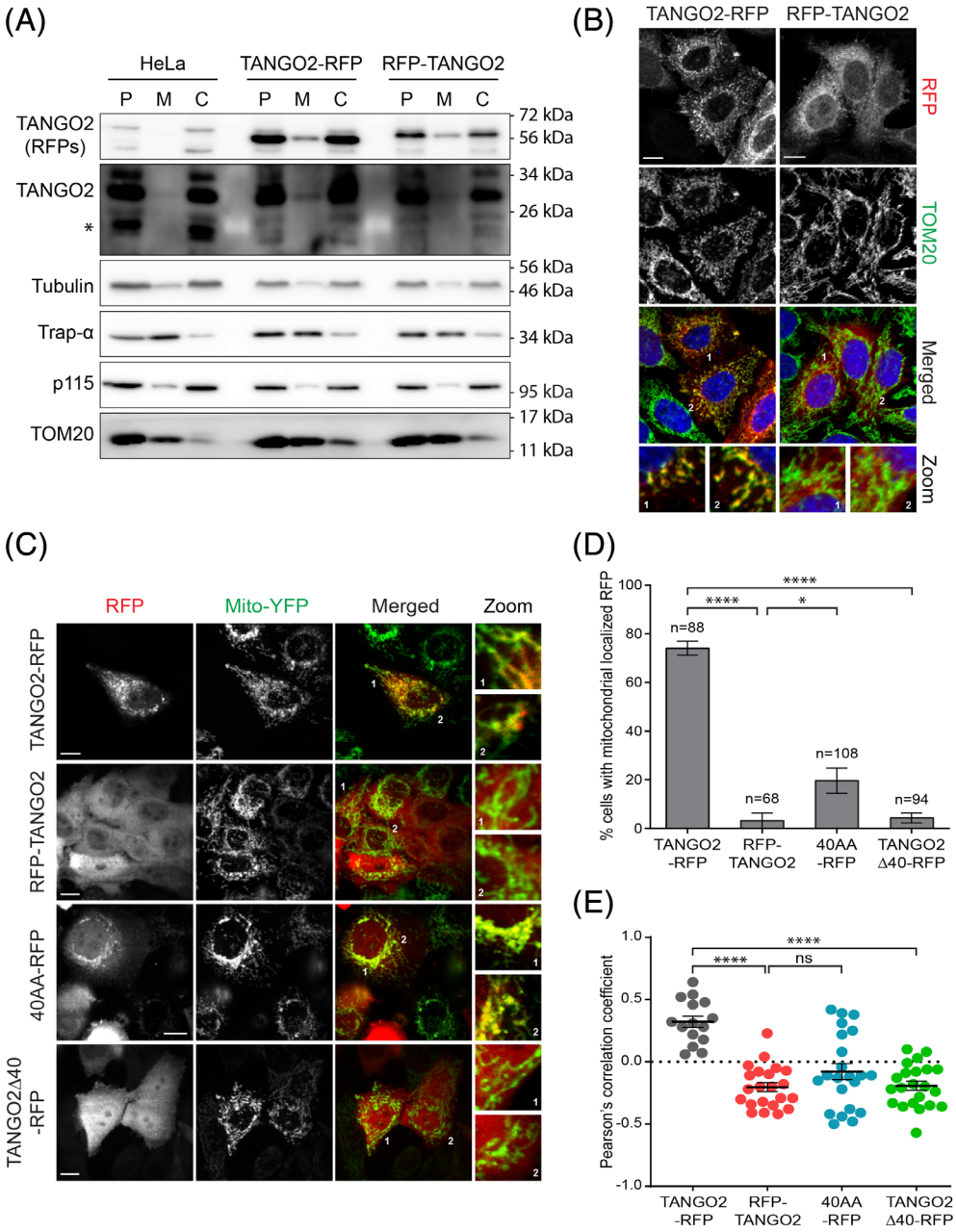

FIGURE 2 A portion of TANGO2 localizes to mitochondria. A, HeLa cells either untransfected or expressing TANGO2-RFP or RFP-TANGO2 were lysed and the resulting lysate (P) was fractionated into a mitochondrial-enriched fraction (M) and a cytosolic fraction (C). Samples were normalized to volume and then probed by western analysis for the indicated proteins. The band with an asterisk (*) in the TANGO2 (endogenous) blot is a cross-reactive polypeptide since it does not disappear upon RNA interference (not shown). B, HeLa cells were transfected with either TANGO2-RFP or RFP-TANGO2. The cells were fixed and stained for RFP using anti-mCherry IgG and for TOM20. The scale bars represent 10 μm. C, HeLa cells stably expressing mitochondrial-localized yellow fluorescent protein (mito-YFP) were transfected with either TANGO2-RFP, RFP-TANGO2, TANGO2Δ40-RFP or RFP fused to the first 40 amino acids of TANGO2 (40AA-RFP) as indicated. The cells were examined by live-cell imaging for the RFP constructs (red channel) or mitochondria (green channel). The scale bars represent 10 μm. D, The percentage of cells from panel (C) that showed localization of the red signal with mitochondria (represented by a green signal in the images) was determined. E, A Pearson's coefficient was determined for the cells in panel (C) to measure the degree of overlap between the mitochondrial and TANGO2 signals. N values are displayed above each bar in panels (D) and (E). **** indicates $P < .0001$ and * indicates $P = .01$

in the mitochondrial fraction, suggesting that the fusion protein might be more stable than the endogenous protein.

In order to determine if the small amounts of fluorescently tagged TANGO2 were residing on membranes or were from cytosolic contaminants, we examined their

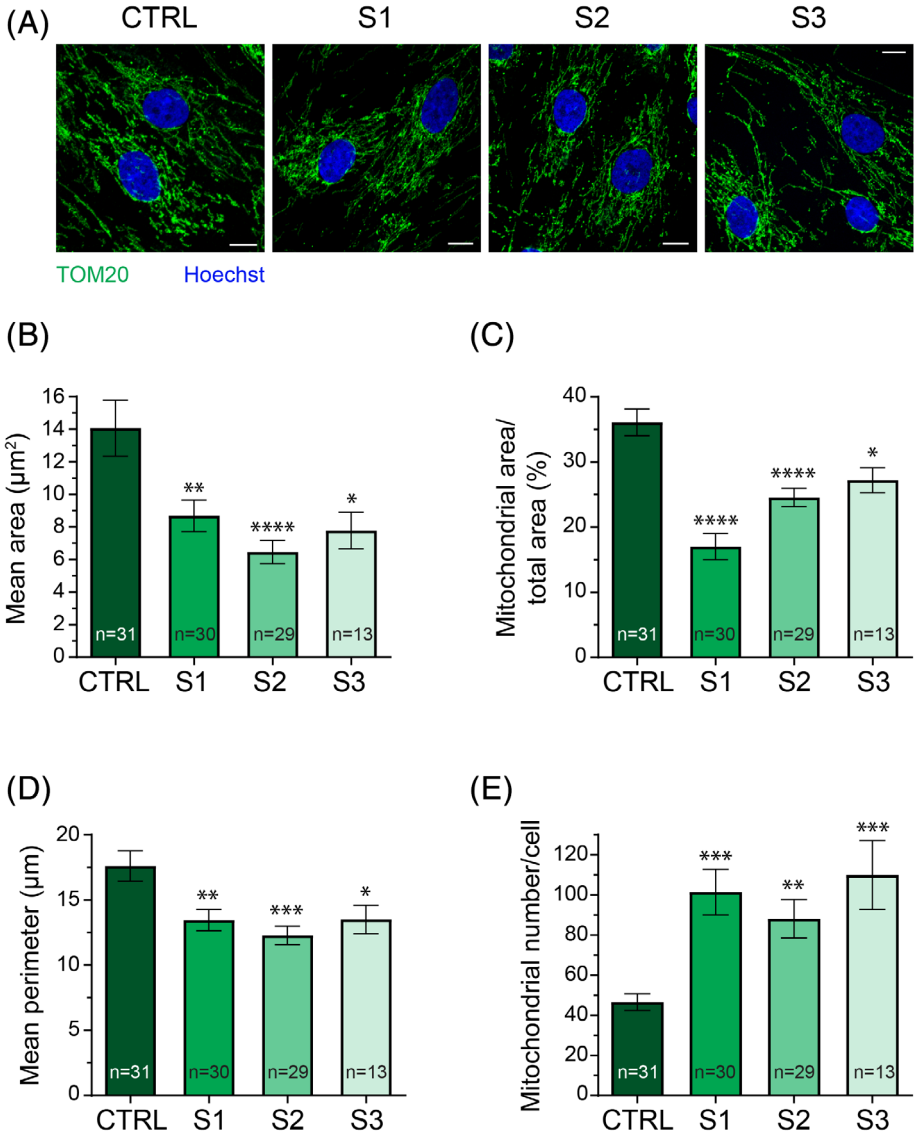

FIGURE 3 Mitochondrial morphology is altered in cells devoid of TANGO2. Fibroblasts from subjects 1-3 as well as control were fixed and stained with anti-TOM20 to reveal mitochondria. Measurements were performed using a custom-designed plugin for Image J that was based upon measurements reported by Valente et al.[11] N values are displayed within each bar in panels (B)-(E). The scale bar represents 10 µm. *$P = .05$, **$P = .005$, ***$P = .0002$, ****$P < .0001$

localization by fluorescence microscopy. When expressed in HeLa cells TANGO2-RFP showed a distinct fluorescence pattern that did not resemble either the ER or the Golgi (Figure 2B). When co-stained with the mitochondrial marker TOM20 we found extensive co-localization between the two proteins, suggesting that some of the TANGO2 protein localized to the mitochondria (Figure 2B). In contrast, RFP-TANGO2 showed diffuse cellular staining with no detectable mitochondrial localization (Figure 2B) nor any significant overlap with the ER marker (Figure S4). Taken together with the cellular fractionation, we conclude that a portion of TANGO2 localizes to the mitochondria but not to a significant degree with the ER or Golgi.

Since TANGO2-RFP but not RFP-TANGO2 localized to the mitochondria, this suggested that a determinant in the amino terminus of the protein was responsible for the mitochondrial localization which was blocked in the RFP-TANGO2 construct. Careful examination of the amino-terminal region of TANGO2 revealed a short stretch of ~30 amino acids that were predicted by MitoProt II[14] to have a high probability of being a mitochondrial targeting sequence. To verify that this stretch of amino acids was important for mitochondrial localization, we compared the mitochondrial localization of TANGO2-RFP to a construct lacking the first 40 amino acids (TANGO2Δ40-RFP) in HeLa cells. Nearly 80% of cells expressing TANGO2-RFP showed mitochondrial localization of the construct while only ~5% of cells expressing RFP-TANGO2 showed mitochondrial localization (Figure 2A,C,D). Removal of the amino-terminal 40 amino acids from TANGO2-RFP (TANGO2Δ40-RFP) resulted in a significant reduction in cells that showed mitochondrial localization to levels approximating those of RFP-TANGO2 (Figure 2C,D). Appending these 40 amino acids to RFP resulted in a significant increase in the number of cells displaying fusion protein that localized to the mitochondria but not to the levels seen

for TANGO2-RFP (Figure 2C,D). A Pearson's coefficient, examining the degree of colocalization between the fluorescently tagged TANGO2 proteins and the mitochondria showed similar results (Figure 2E). We also assessed the amount of fluorescently tagged TANGO2 that was mitochondrially localized in the cells by examining the ratio of the signal on mitochondria compared to that within the cytosol (Figure S5). The results were consistent with mitochondrial localization of TANGO2-RFP compared to the TANGO2Δ40-RFP construct. These results suggest that the 40 amino-terminal residues of TANGO2 are necessary, but not sufficient, for mitochondrial localization of the protein.

3.3 | Mitochondrial morphology is altered in cells devoid of TANGO2

Since some TANGO2 protein localized to the mitochondria, we asked whether there were any detectable changes in mitochondrial morphology in cells derived from the individuals with TANGO2 variants compared to control. The cells were stained for TOM20 to reveal the mitochondrial network (Figure 3A). A script was then created to allow for the measurement of various mitochondrial parameters in the software Image J including mean area, percentage of mitochondria area compared to the whole cell, mitochondria perimeter, and mitochondria number per cell (Figure 3B-E). There was a significant decrease in mean mitochondria area in fibroblasts from all three individuals with TANGO2 variants compared to control (Figure 3B). Similarly, significant decreases in percentage of total cell area occupied by mitochondria, perimeter of the mitochondria and increase in the number of mitochondria per cell were also seen in all three individuals compared to control (Figure 3C-E). Therefore, these measurements suggest a change in mitochondrial morphology in cells devoid of TANGO2 and are consistent with the localization of the protein to mitochondria.

4 | DISCUSSION

Here we provide evidence suggesting that TANGO2 plays a role in two distinct cellular processes: ER-to-Golgi traffic and mitochondrial morphology. The effect on mitochondrial morphology suggests that the protein may affect an as yet undetermined function at this organelle. The fibroblasts used in this study all harbor TANGO2 variants that either result in a homozygous deletion of exons 3-9, a compound heterozygous variant consisting of deletion of exons 3-9 with a p.Cys2Alafs*35 variant, and a homozygous p.Arg140* variant. While originally identified in a *Drosophila* screen for genes whose products function in the endomembrane system, TANGO2 was proposed to function in Golgi organization.[3] However, a role in this process outside of the *Drosophila* model system was never demonstrated. Several studies attempted to show such a function but results have been enigmatic (Table 1). Consistent with one study that showed no redistribution of mannosidase II to the ER in individuals with either a deletion encompassing exons 4-6 or harboring a p.His94Thrfs*3 frameshift variant,[6] we also did not see a change in localization of this Golgi enzyme nor in the Golgi matrix marker p115 in fibroblasts from the three individuals studied here, expanding this result to three other *TANGO2* genotypes. It remains to be seen if these findings also hold true for other TANGO2 variants including missense variants.

While the mitochondrial localization was not completely unexpected given the clinical features of individuals with *TANGO2* variants (see below), it is an area that has been clouded by conflicting results, especially in light of its purported role in membrane traffic. The *Drosophila* protein was reported to localize to the cytosol and the Golgi and depletion of the protein caused a redistribution of a Golgi enzyme back to the ER. We found no evidence of Golgi localization for the human protein but did show a significant TANGO2-dependent delay in ER-to-Golgi traffic. Another study examined retrograde transport from the Golgi to the ER and found a slight delay in this pathway in fibroblasts derived from individuals with a hemizygous p.Phe5del variant,[7] though TANGO2 dependence was not demonstrated. A decrease in ER and Golgi surface area and an increase in ER stress was reported in a different study in individuals with a homozygous p.Gly154Arg variant.[2] Interestingly, in most cases where a protein that functions in ER-to-Golgi traffic is depleted, there is usually a profound change in the morphology of the Golgi. TANGO2 seems to be unique in that its absence disrupts this pathway yet the Golgi appears morphologically normal by light microscopy. This might be indicative of a role at ER membranes that indirectly influences ER-to-Golgi traffic. In this scenario TANGO2 may be transiently recruited to membranes much like other proteins involved in membrane traffic such as N-ethylmaleiminde sensitive factor (NSF) and soluble NSF attachment protein receptor (SNAP), thus accounting for our inability to detect the protein at ER or Golgi membranes.

On the other hand, a study that examined three TANGO2 isoforms including the canonical one did not find evidence for either Golgi or mitochondrial localization, concluding that the protein was cytosolic.[6] It is noteworthy that the former study did in fact report an

TABLE 1 Mitochondrial and endomembrane trafficking defects in TANGO2 variants

	TANGO2 variant[a]							
	Homozygous c.418C>T	**Homozygous c.[(56þ1_57–1)_(*1_?)del]**	**Exon 3-9 del; exon 6 del**	**c.[4delT];[(56þ1_57-1)_(*1_?)del] p.[Cys2Alafs*35];[?]**	**Homozygous c.460G>A**	**Homozygous c.605+1C>G**	**Homozygous c.280delC**	**Hemizygous c.11_13delTCT**
ER-Golgi traffic	Delayed from ER to Golgi	Delayed from ER to Golgi	Delayed from ER to Golgi	Delayed from ER to Golgi	Not assessed	Not assessed	Not assessed	Delayed BFA-induced Golgi disassembly
Other endomembrane alterations	None detected	None detected	None detected	None detected	Reduced ER and Golgi volume, increased ER stress	Not assessed	None detected	Not assessed
Mitochondrial defects	More abundant and shorter, mild reduction in complex I activity, reduction in palmitate-dependent respiration	More abundant and shorter	More abundant and shorter	More abundant and, shorter	Not assessed	Electron transport chain enzyme activity did not meet criteria for respiratory chain disorder	Normal morphology and membrane potential for fibroblasts, prominent mitochondria that were slightly enlarged and rounded in muscle, impaired oxygen consumption, reduced complex II activity	No ragged red fibers or COX-deficient fibers in muscle, multiple deficiencies in mitochondrial respiratory chain enzyme activities and reduced CoQ_{10} in muscle, increase in all oxidative phosphorylation complexes in fibroblasts
Localization	Mitochondria, cytosol	Mitochondria, cytosol	Mitochondria, cytosol	Not assessed	Not assessed	Not assessed	Cytosol (all isoforms with alternative amino-terminal sequences)	Not assessed
Metabolic/laboratory abnormalities	*Elevated*: TSH, plasma lactate, CK, acyl carnitines, dicarboxylic acids, ketones in urine reduced: blood sugar	*Elevated*: TSH, plasma lactate (mild), CK, acyl carnitines (mild),ketones in urine *reduced*: blood sugar	*Elevated*: TSH, CK plasma lactate, ketones in urine *reduced*: blood sugar	*Elevated*: TSH, plasma lactate, CK, acyl carnitines, dicarboxylic acids, ketones in urine *reduced*: blood sugar	*Elevated*: lactate, CPK, AST, ALT *reduced*: blood sugar	*Elevated*: CPK *reduced*: blood sugar	*Elevated*: TSH *reduced*: blood sugar	*Elevated*: ALT, AST, CK, lactate, ketones in urine *reduced*: blood sugar
Reference	This study and Kremer et al[1]	This study and Kremer et al[1]	This study and Dines et al[15]	Kremer et al[1]	Lalani et al[2]	Sen et al[16]	Jennions et al[6]	Mingirulli et al[7]

Abbreviations: AST, aspartate aminotransferase; ALT, alanine aminotransferase; BFA, brefeldin A; CK, creatine kinase, CPK, creatine phosphokinase; TSH, thyroid stimulating hormone.
[a]Only variants in which localization, trafficking or mitochondrial enzyme activity were examined are reported.

increase in mitochondrial localization of nearly four-fold for the GFP-tagged canonical form compared to GFP alone. Although Kremer and co-workers did not localize the protein, they did report a decrease in palmitate-dependent oxygen consumption, concluding that there may be a defect in electron transfer to the mitochondrial respiratory chain.[1] This conclusion was supported by a direct assay of mitochondrial respiratory complexes that showed a mild decrease in the activity of several of the complexes[6,7] as well as changes in the levels of some of the complexes.[7] In a single study of mouse TANGO2 (referred to as T10), mitochondrial localization was demonstrated.[5] Of note is the fact that the first 30 amino acids of mouse TANGO2 are identical to the human canonical isoform. Our findings show a clear mitochondrial localization for TANGO2, mitochondrial morphological changes and a significant delay in ER-to-Golgi traffic with these specific TANGO2 variants. This study unifies the disparate localization and functional findings of earlier studies and suggests that there are at least two pools of TANGO2 that independently or jointly play a role in both ER-to-Golgi traffic and mitochondrial organization and perhaps function. An intriguing possibility is that TANGO2 may affect cellular energy levels which are predicted to affect membrane traffic. We noted an exacerbation of the trafficking defect in the fibroblasts upon 12 hours of glucose starvation (MPM and MS, unpublished observation), consistent with this notion. This result is also consistent with the diet-induced metabolic crises seen in some individuals with TANGO2 variants.

Although TANGO2 does not appear in MitoCarta2.0, a catalog of reported mitochondrial proteins,[17] its absence can be explained in a number of ways. First, the levels of TANGO2 may be such that it has escaped detection thus far. In this respect it is notable that TANGO2 was not detected in a comparative proteomic analysis of control and TANGO2-deficient fibroblasts.[7] Second, its mitochondrial localization may be regulated depending on cellular conditions. Third, it may peripherally associate with the organelle and fall off during some preparations. The latter notion may explain the difference we see by cellular fractionation, where only small amounts are seen in the mitochondrial fraction, compared to fluorescence microscopy where a substantial portion of the TANGO2-RFP signal readily overlaps with mitochondria. Finally, we examined the amino-terminal 40 residues of the canonical isoform of TANGO2. There are a number of other TANGO2 isoforms that differ at the amino-terminus and are not predicted to have a mitochondrial targeting sequence and these forms may be the predominant forms in cells, a notion that needs further analysis.

The dual role of TANGO2 in membrane traffic and at the mitochondria is consistent with the complex phenotype seen in individuals with TANGO2 variants. On the one hand, these individuals suffer from recurrent rhabomyolysis.[18] A similar phenotype was recently reported for individuals harboring TRAPPC2L variants.[19] TRAPPC2L is a component of the TRAPP complex[20] that has a well-established role in membrane traffic, particularly in ER-to-Golgi traffic.[21,22] On the other hand, individuals with TANGO2 variants also present with recurrent metabolic crises, muscle weakness, cardiac arrhythmia, and laboratory findings consistent with defects in mitochondrial fatty acid oxidation,[18] a process that could have profound effects on cellular energy levels. These features show some overlap with individuals suffering from deficiency in either carnitine palmitoyl transferase 2 or VLCAD,[8,23] cellular processes that are carried out in mitochondria.

In summary, our study harmonizes findings in the burgeoning field of TANGO2 biology and highlights the need to study the function of this protein in both mitochondrial physiology and ER-to-Golgi traffic. Understanding which residues in the protein affect these cellular processes will also allow better predictions of the expected phenotypes. Present work is now focused on identifying the protein interaction network for TANGO2 as well as a proteomic profiling of cells devoid of the protein to better understand the role that TANGO2 plays in these processes.

ACKNOWLEDGEMENTS

All microscopy was performed at the Centre for Microscopy and Cellular Imaging at Concordia University. M.S is supported by research grants from the Canadian Institutes of Health Research and the Natural Sciences and Engineering Research Council (Canada). FD is supported by a research grant of the German Research Foundation/ Deutsche Forschungsgemeinschaft (DI 1731/2-2). T.K. and F.D. are supported by the German Federal Ministry of Education and Research (BMBF, Bonn, Germany) through a grant to the German Network for Mitochondrial Disorders (mitoNET, 01GM1906A). The support of the TANGO2 Research Foundation to M.S. and F.D. is gratefully acknowledged. The authors also gratefully acknowledge the family of Louisa Sophie Kuhlmann, which supported this work through fundraising. The authors confirm independence from the sponsors; the content of the article has not been influenced by the sponsors.

CONFLICT OF INTEREST

The authors declare no conflicts of interest.

AUTHOR CONTRIBUTIONS

Miroslav P. Milev performed all microscopy, biochemical experiments with the exception of Figures 1A and S1, statistical analyses, analyzed data and interpreted the results, prepared all the figures and edited the manuscript; Djenann Saint-Dic assisted in the biochemical experiments and edited the manuscript; Khashayar Zardoui generated RFP-tagged TANGO2 constructs and edited the manuscript; Thomas Klopstock provided a TANGO2 cell line and edited the manuscript; Christopher Law wrote the scripts for the mitochondrial morphology measurements and for the mitochondrial vs non-mitochondrial TANGO2 fraction and edited the manuscript; Michael Sacher and Felix Distelmaier designed the study, analyzed the data and wrote the manuscript.

ETHICS STATEMENT

The use of patient-derived fibroblasts was approved by the ethic committee of the Heinrich-Heine university (study number 6067R). No human subjects were used in this study.

All procedures followed were in accordance with the ethical standards of the responsible committee on human experimentation (institutional and national) and with the Helsinki Declaration of 1975, as revised in 2000 (5). Informed consent was obtained from the parents of all patients for being included in the study.

ORCID

Michael Sacher https://orcid.org/0000-0003-2926-5064

REFERENCES

1. Kremer LS, Distelmaier F, Alhaddad B, et al. Bi-allelic truncating mutations in TANGO2 cause infancy-onset recurrent metabolic crises with encephalocardiomyopathy. *Am J Hum Genet*. 2016;98:358-362.
2. Lalani SR, Liu P, Rosenfeld JA, et al. Recurrent muscle weakness with rhabdomyolysis, metabolic crises, and cardiac arrhythmia due to bi-allelic TANGO2 mutations. *Am J Hum Genet*. 2016;98:347-357.
3. Bard F, Casano L, Mallabiabarrena A, et al. Functional genomics reveals genes involved in protein secretion and Golgi organization. *Nature*. 2006;439:604-607.
4. Saito K, Chen M, Bard F, et al. TANGO1 facilitates cargo loading at endoplasmic reticulum exit sites. *Cell*. 2009;136:891-902.
5. Maynard TM, Meechan DW, Dudevoir ML, et al. Mitochondrial localization and function of a subset of 22q11 deletion syndrome candidate genes. *Mol Cell Neurosci*. 2008;39:439-451.
6. Jennions E, Hedberg-Oldfors C, Berglund AK, et al. TANGO2 deficiency as a cause of neurodevelopmental delay with indirect effects on mitochondrial energy metabolism. *J Inherit Metab Dis*. 2019;42:898-908.
7. Mingirulli N, Pyle A, Hathazi D, et al. Clinical presentation and proteomic signature of patients with TANGO2 mutations. *J Inherit Metab Dis*. 2019;43:297–308.
8. Longo N, Amat di San Filippo C, Pasquali M. Disorders of carnitine transport and the carnitine cycle. *Am J Med Genet C Semin Med Genet*. 2006;142C:77-85.
9. Boncompain G, Divoux S, Gareil N, et al. Synchronization of secretory protein traffic in populations of cells. *Nat Methods*. 2012;9:493-498.
10. Milev MP, Grout ME, Saint-Dic D, et al. Mutations in TRAPPC12 manifest in progressive childhood encephalopathy and Golgi dysfunction. *Am J Hum Genet*. 2017;101:291-299.
11. Milev MP, Stanga D, Schanzer A, et al. Characterization of three TRAPPC11 variants suggests a critical role for the extreme carboxy terminus of the protein. *Sci Rep*. 2019;9:14036.
12. Valente AJ, Maddalena LA, Robb EL, Moradi F, Stuart JA. A simple ImageJ macro tool for analyzing mitochondrial network morphology in mammalian cell culture. *Acta Histochem*. 2017;119:315-326.
13. Soubannier V, Rippstein P, Kaufman BA, Shoubridge EA, McBride HM. Reconstitution of mitochondria derived vesicle formation demonstrates selective enrichment of oxidized cargo. *PLoS One*. 2012;7:e52830.
14. Claros MG, Vincens P. Computational method to predict mitochondrially imported proteins and their targeting sequences. *Eur J Biochem*. 1996;241:779-786.
15. Dines JN, Golden-Grant K, LaCroix A, et al. TANGO2: expanding the clinical phenotype and spectrum of pathogenic variants. *Genet Med*. 2019;21:601-607.
16. Sen K, Hicks MA, Huq AHM, Agarwal R. Homozygous TANGO2 single nucleotide variants presenting with additional manifestations resembling alternating hemiplegia of childhood-expanding the phenotype of a recently reported condition. *Neuropediatrics*. 2019;50:122-125.
17. Calvo SE, Clauser KR, Mootha VK. MitoCarta2.0: an updated inventory of mammalian mitochondrial proteins. *Nucleic Acids Res*. 2016;44:D1251-D1257.
18. Lalani SR, Graham B, Burrage L, et al. TANGO2-related metabolic encephalopathy and arrhythmias. In: Adam MP, Ardinger HH, Pagon RA, et al., eds. *GeneReviews([R])*. University of Washington: Seattle, WA; 2018.
19. Milev MP, Graziano C, Karall D, et al. Bi-allelic mutations in TRAPPC2L result in a neurodevelopmental disorder and have an impact on RAB11 in fibroblasts. *J Med Genet*. 2018;55:753-764.
20. Scrivens PJ, Shahrzad N, Moores A, Morin A, Brunet S, Sacher M. TRAPPC2L is a novel, highly conserved TRAPP-interacting protein. *Traffic*. 2009;10:724-736.
21. Sacher M, Kim YG, Lavie A, Oh BH, Segev N. The TRAPP complex: insights into its architecture and function. *Traffic*. 2008;9:2032-2042.
22. Kim JJ, Lipatova Z, Segev N. TRAPP complexes in secretion and autophagy. *Front Cell Dev Biol*. 2016;4:20.

23. Andresen BS, Olpin S, Poorthuis BJ, et al. Clear correlation of genotype with disease phenotype in very-long-chain acyl-CoA dehydrogenase deficiency. *Am J Hum Genet*. 1999;64: 479-494.

SUPPORTING INFORMATION

Additional supporting information may be found online in the Supporting Information section at the end of this article.

How to cite this article: Milev MP, Saint-Dic D, Zardoui K, et al. The phenotype associated with variants in *TANGO2* may be explained by a dual role of the protein in ER-to-Golgi transport and at the mitochondria. *J Inherit Metab Dis*. 2020;1–12. https://doi.org/10.1002/jimd.12312

Suppl. Figure 1

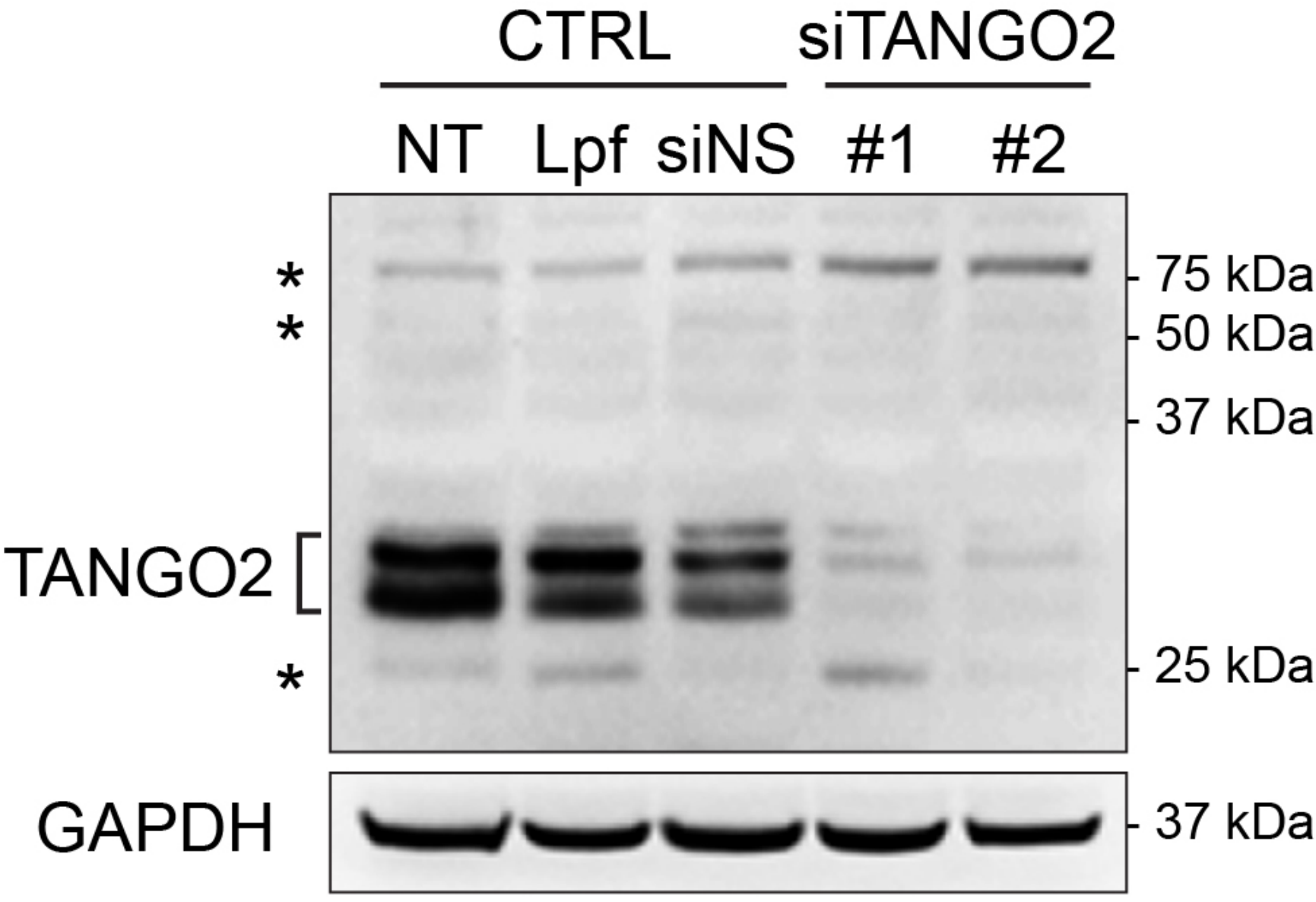

Suppl. Figure 2

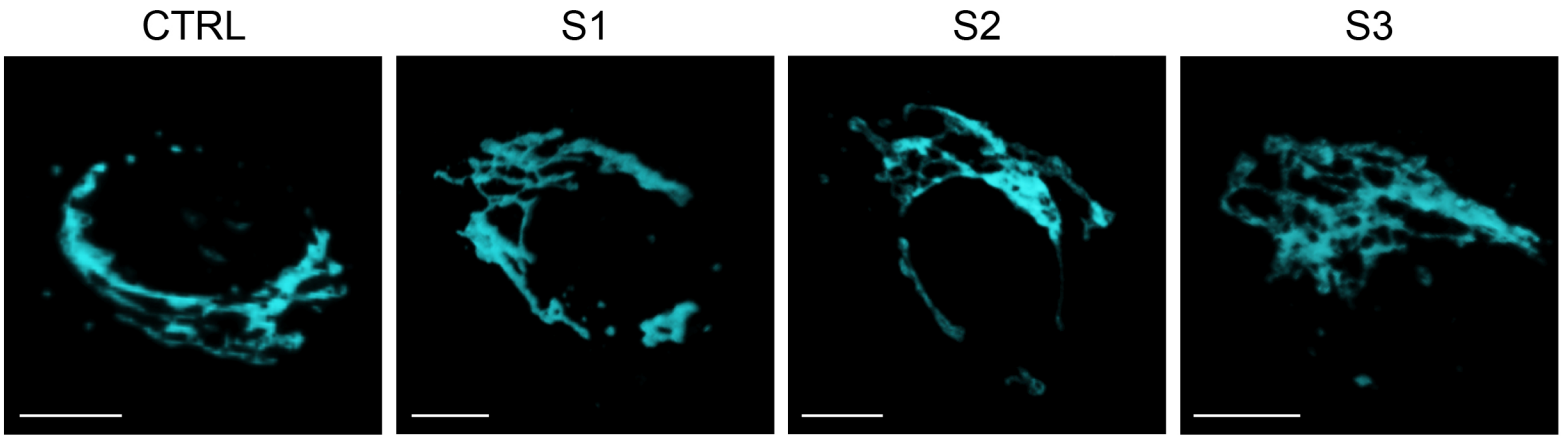

Suppl. Figure 3

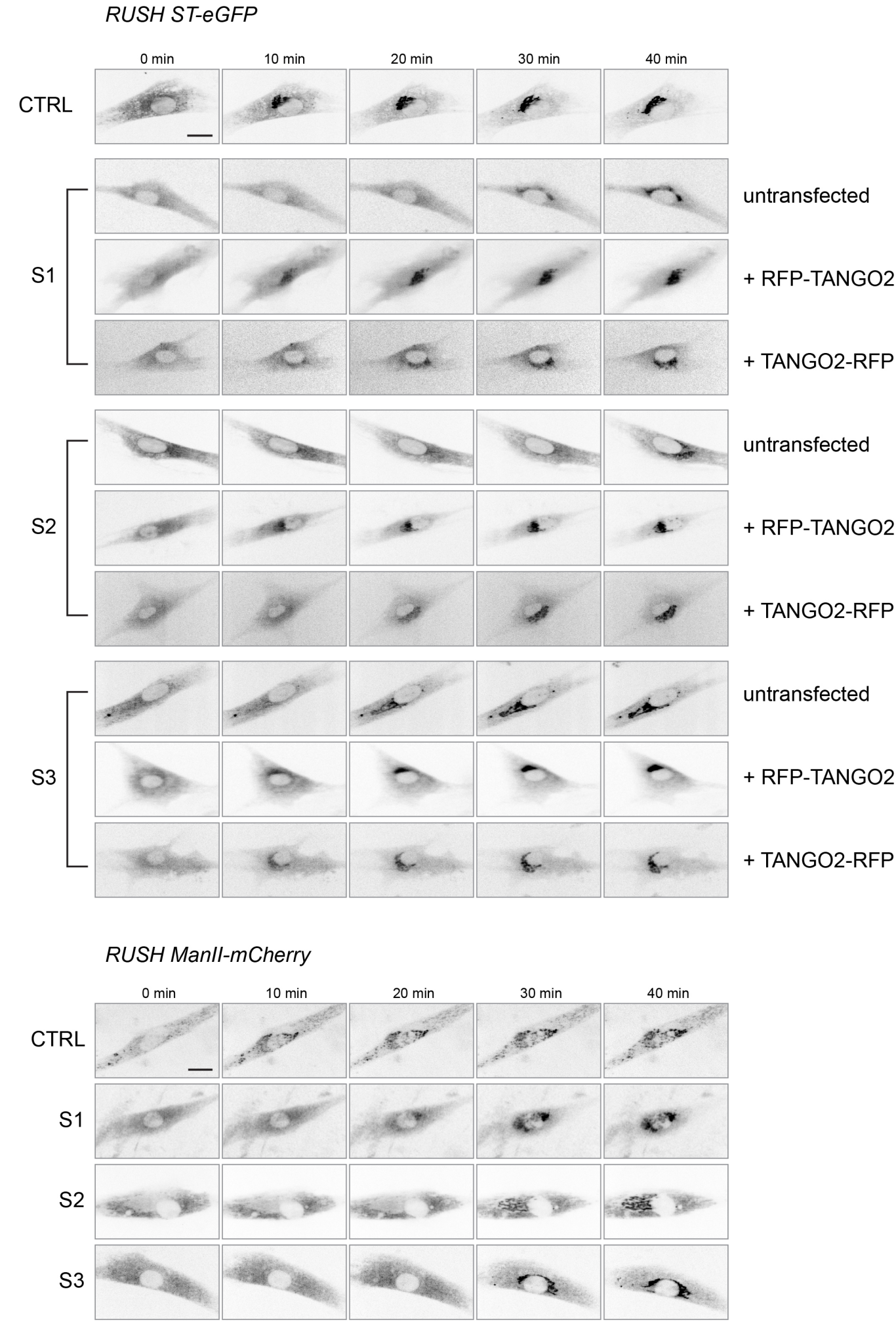

Suppl. Figure 4

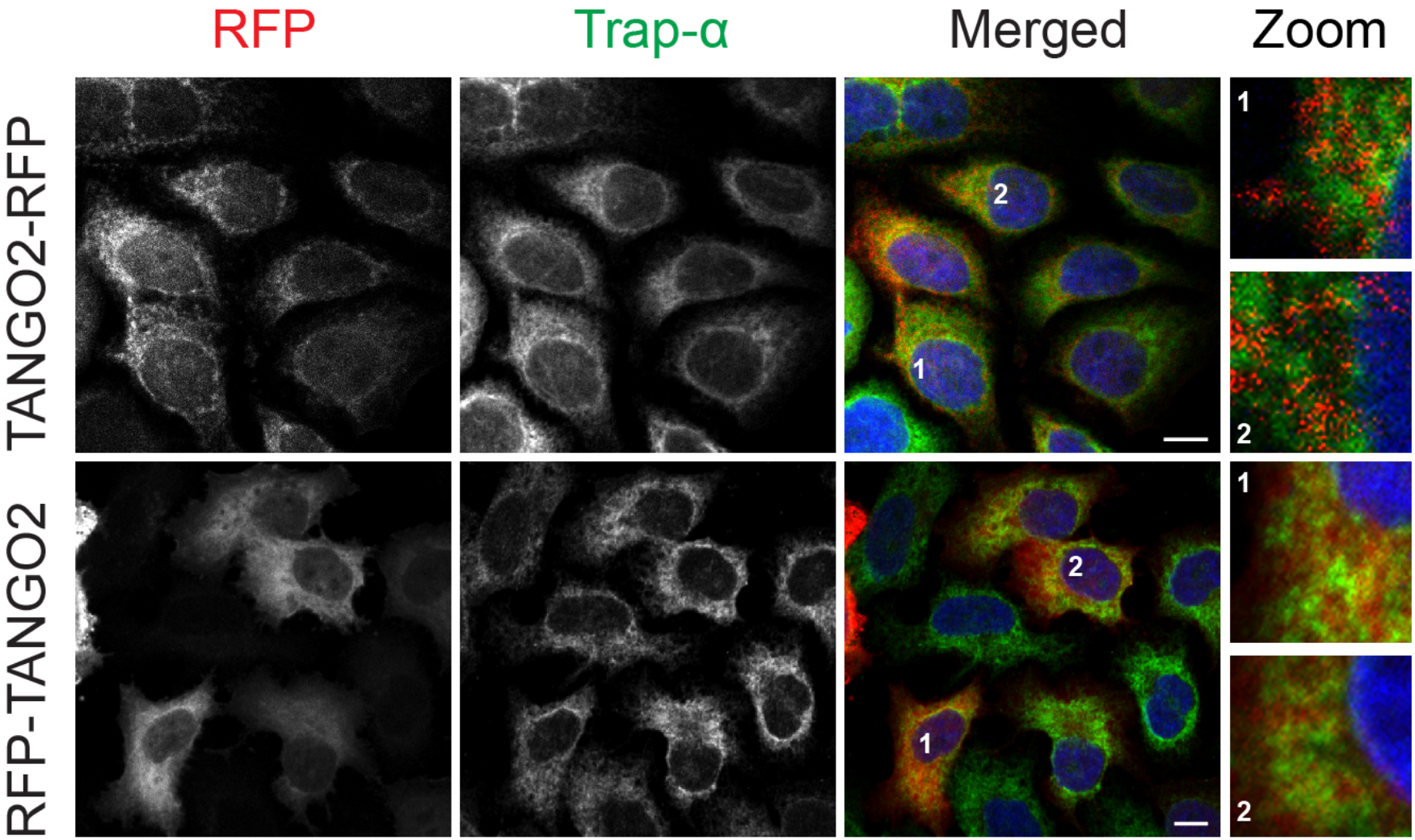

Suppl. Figure 5